Sp8 and *Sp9*, two closely related *buttonhead*-like transcription factors, regulate *Fgf8* expression and limb outgrowth in vertebrate embryos

Yasuhiko Kawakami[1], Concepción Rodríguez Esteban[1], Takaaki Matsui[1], Joaquín Rodríguez-León[2], Shigeaki Kato[3] and Juan Carlos Izpisúa Belmonte[1,*]

[1]Gene Expression Laboratory, The Salk Institute for Biological Studies, La Jolla, CA 92037-1099, USA
[2]Unidade de Desenvolvimento, Instituto Gulbenkian de Ciencia, Rua Da quinta Grande 6 Aptdo 14. 2780-901 Oeiras, Portugal
[3]The Institute of Molecular and Cellular Biosciences, The University of Tokyo, 1-1-1 Yayoi, Bunkyo-ku, Tokyo, 113-0032, Japan
*Author for correspondence (e-mail: belmonte@salk.edu)

Accepted 28 June 2004

Development 131, 4763-4774
Published by The Company of Biologists 2004
doi:10.1242/dev.01331

Summary

Initiation and maintenance of signaling centers is a key issue during embryonic development. The apical ectodermal ridge, a specialized epithelial structure and source of Fgf8, is a pivotal signaling center for limb outgrowth. We show that two closely related *buttonhead*-like zinc-finger transcription factors, *Sp8* and *Sp9*, are expressed in the AER, and regulate *Fgf8* expression and limb outgrowth. Embryological and genetic analyses have revealed that *Sp8* and *Sp9* are ectodermal targets of Fgf10 signaling from the mesenchyme. We also found that Wnt/β-catenin signaling positively regulates *Sp8*, but not *Sp9*. Overexpression functional analyses in chick unveiled their role as positive regulators of *Fgf8* expression. Moreover, a dominant-negative approach in chick and knockdown analysis with morpholinos in zebrafish revealed their requirement for *Fgf8* expression and limb outgrowth, and further indicate that they have a coordinated action on *Fgf8* expression. Our study demonstrates that *Sp8* and *Sp9*, via *Fgf8*, are involved in mediating the actions of Fgf10 and Wnt/β-catenin signaling during vertebrate limb outgrowth.

Key words: Apical ectodermal ridge, Sp transcription factor, *Fgf8*, *Fgf10*, Wnt, Vertebrate limb

Introduction

Understanding the molecular mechanisms that control how outgrowth of different tissues and organs of the embryo are established and maintained is one of the major questions in the study of embryonic development. The advent of molecular and genetic techniques have provided powerful tools with which to dissect the ways in which transcription factors and signaling molecules are used to allow neighboring cells to communicate and adopt positional information, which are provided by the action of embryonic signaling centers. The signaling centers direct the primordia of tissues and organs towards outgrowth and pattern formation for proper morphogenesis. Formation and maintenance of signaling centers should be tightly regulated, spatially and temporally, in order for them to control tissue development properly. Although there are many different model systems in which, by the action of signaling centers, molecular and genetic mechanisms of outgrowth have been studied, the vertebrate limb is one of the best-understood models.

Limb outgrowth requires the formation and maintenance of three different signaling centers: the apical ectodermal ridge (AER) controls proximodistal growth; the zone of polarizing activity, which is located in the posterior mesenchyme is responsible for anteroposterior pattern formation; and the non-ridge ectoderm directs formation of the dorsoventral axis. Their coordinated action constructs the three-dimensional morphology of the limb (reviewed by Capdevila and Izpisua Belmonte, 2001; Niswander, 2003; Tickle, 2002a). Among these signaling centers in the limb bud, the AER, which is a thickened epithelial structure positioned at the distal edge of the limb bud at the dorsoventral boundary, is pivotal for maintaining limb outgrowth. Surgical removal of the AER results in cell death in the mesenchyme and abrogates limb outgrowth (Dudley et al., 2002; Rowe et al., 1982; Sun et al., 2002). The importance and necessity of the AER in limb outgrowth is a conserved feature of vertebrate development as illustrated in mice, chick and zebrafish (Grandel and Schulte-Merker, 1998; Tickle, 2002b). Despite recent extensive studies, the molecular and genetic mechanisms that control initiation and maintenance of the AER in these model organisms is far from being understood.

The morphogenesis of the AER can be divided into two processes.

(1) The induction of AER precursor cells in the surface ectoderm that will migrate toward the dorsoventral boundary and form the AER. These cells start to express fibroblast growth factor 8 (*Fgf8*), a member of the Fgf superfamily that acts as an essential signaling molecule involved in vertebrate limb outgrowth (Crossley et al., 1996b; Lewandoski et al., 2000; Moon and Capecchi, 2000; Vogel et al., 1996).

(2) Maturation of the AER that results in formation of the characteristic, thickened structure (Loomis et al., 1998). The

initial induction of AER precursor cells depends on the activity of Fgf10 emanating from the lateral plate mesoderm (Min et al., 1998; Ohuchi et al., 1997; Sekine et al., 1999). In the absence of *Fgf10*, no *Fgf8* expression is detected, indicating that induction of the AER precursor cells does not take place, and the AER is not formed.

In addition, ectodermal Wnt/β-catenin signaling and Bmp signaling are essential for induction of *Fgf8* expression in AER precursors (Ahn et al., 2001; Barrow et al., 2003; Kengaku et al., 1998; Pizette et al., 2001; Soshnikova et al., 2003). The AER precursors migrate to the dorsoventral boundary, and form a structurally distinguishable AER by apical compaction (Loomis et al., 1998). Secreted from the AER, Fgf8 signals to the underlying mesenchyme, and Fgf10 produced by the distal mesenchyme in turn signals to the AER, resulting in establishment of the reciprocal positive feedback loop that maintains the expression of each one (Ohuchi et al., 1997; Xu et al., 1998). This positive-feedback loop, mediated by different splicing isoforms of *Fgfr2* (Arman et al., 1999; Ornitz et al., 1996), maintains the AER and limb outgrowth. Further studies have shown that Wnt/β-catenin activity is also required for maintaining *Fgf8* expression in the AER (Barrow et al., 2003; Kawakami et al., 2001; Soshnikova et al., 2003). Our current understanding of AER development implies that the concerted signaling of these and possibly other growth factors leads to the activation of different transcription factors that in turn elicit the instructions that permit proper limb development.

Among the different transcription factors involved in these processes, it was recently shown, by gene targeting analysis, that *Sp8*, a *buttonhead* (*btd*)-like zinc (Zn) finger transcription factor is required for maintaining, but not for initial induction of *Fgf8* expression in AER precursor cells (Bell et al., 2003; Treichel et al., 2003). The Sp family of transcription factors is united by a particular combination of a C2H2 type Zn-finger DNA-binding domain and *btd* domain (Bouwman and Philipsen, 2002; Philipsen and Suske, 1999). Eight Sp members have been identified in mouse and human. Although the necessity of *Sp8* for mouse limb outgrowth has been reported, it is largely unknown how *Sp8* interacts with the previously mentioned signaling pathways to maintain limb outgrowth. For example, although Fgf10, Wnt/β-catenin and Sp8 are factors that are required for AER maintenance and subsequent limb outgrowth, it is not clear whether they are sufficient or if other factors are also required.

To gain further insights into the role of Sp genes during vertebrate limb development, we have performed several experiments. They include the isolation of a novel *btd*-like Zn-finger transcription factor, *Sp9*. *Sp9* contains a *btd* domain and Zn-finger domain that are highly homologous to those of *Sp8*. Using mouse, chick and zebrafish embryos, we have studied the embryonic expression pattern, regulation and role of *Sp8* and *Sp9* during limb development. Both *Sp8* and *Sp9* are expressed in the AER, but regulated differently by Wnt and Fgf signaling. Loss- and gain-of-function approaches revealed that both *Sp8* and *Sp9* positively regulate *Fgf8* expression in the AER and contribute to limb outgrowth in vertebrate embryos.

Materials and methods

Cloning of *Sp8* and *Sp9* from mouse, chick and zebrafish

Chick *Sp8* and *Sp9* were obtained by screening cDNA libraries. The full-length mouse *Sp8* was obtained by combining an EST clone and a PCR clone, and mouse *Sp9* was obtained as EST clones. Zebrafish *sp8* and *sp9* were obtained by screening a 24-hours post fertilization (hpf) cDNA library (Stratagene) and 5′RACE. The screening of libraries and PCR were carried out by following standard procedures. The nucleotide sequences of chick *Sp8*, chick *Sp9*, mouse *Sp9*, zebrafish *sp8* and zebrafish *sp9* are deposited in GenBank with the Accession Numbers AY591906, AY591907, AY591908, AY591904 and AY591905, respectively.

In situ hybridization and cartilage staining

Chick *Sp8* and *Sp9* probes were derived from a partial open reading frame covering 3′ to the Zn-finger domain and 3′UTR in order to avoid cross hybridization. The mouse *Sp8* probe contains 1 kb of the 3′UTR and the *Sp9* probe contains 750 bp covering the 5′UTR and partial ORF, 5′ to the *btd* domain. Zebrafish *sp8* and *sp9* probes are derived from 3′UTR sequences. Chick *Fgf8* and zebrafish *fgf8* probes have been described previously (Ng et al., 2002; Vogel et al., 1996). Zebrafish *prx1* was cloned by RT-PCR and confirmed by nucleotide sequencing (Accession Number BC053228).

Chick and mouse embryos were examined by whole-mount in situ hybridization and Alcian green cartilage staining as described (Vogel et al., 1996). Zebrafish embryos were examined by whole-mount in situ hybridization as described (Ng et al., 2002).

Mutant mice and zebrafish

Mouse embryos deficient for *Fgf10* (Min et al., 1998; Sekine et al., 1999), *Dkk1* (Mukhopadhyay et al., 2001) and *Lrp6* (Pinson et al., 2000) were used. Zebrafish mutants, *heartstrings* (*hst*) (Garrity et al., 2002; Ng et al., 2002), *neckless* (*nkl*) (Begemann et al., 2001) and *dackel* (*dak*) (Grandel et al., 2000) have been described previously.

Viral production and injection into chick embryos

The full-length mouse *Sp8* and *Sp9* were subcloned into *RCAS* BP(A) vector. In order to construct dominant-active and -negative forms of *Sp8* and *Sp9*, a part of the open reading frame (from the btd domain to the termination codon; *ΔN-Sp8* and *ΔN-Sp9*) was fused to a VP16 activation domain (VP16-) or an Engrailed-repressor domain (EnR-), and subcloned into the *RCAS* BP(A) vector. The dominant-active β-catenin clone has been described previously (Capdevila et al., 1998). Retroviral production was performed as previously described (Vogel et al., 1996). Staging of chick embryos was according to Hamburger and Hamilton (HH; Hamburger and Hamilton, 1951). Prospective limb fields of chick embryos at HH stage 9-11 were infected with the viruses. An *RCAS* BP(A)-alkaline phosphatase virus was used as a control and no phenotypic changes in gene expression or limb morphology were observed. The injected embryos were developed until desired stages and fixed for analysis.

Bead and cell-pellet implantation

Heparin beads were soaked in Fgf10 (1 mg/ml) or Fgf8 (1 mg/ml). AG-X beads were soaked in the Fgf receptor kinase inhibitor SU5402 (Calbiochem), at 2 mg/ml in DMSO. The beads were implanted into stage 19-21 developing chick limb buds as described previously (Kawakami et al., 2003). Chick embryonic fibroblasts were infected with *RCAS* BP(A)-*Wnt3a* (Kengaku et al., 1998), and implanted into limb buds as described previously (Wada et al., 1999). Control beads soaked in PBS or DMSO and chick embryonic fibroblasts with *RCAS* BP(A)-alkaline phosphatase were used at the same stage and no change in gene expression was observed. The manipulated embryos were incubated for desired periods and processed for in situ hybridization analysis.

Morpholino injections

Morpholino oligo nucleotides were designed by and obtained from GeneTools LLC (Eugene, OR). The zebrafish *sp8* morpholino lies

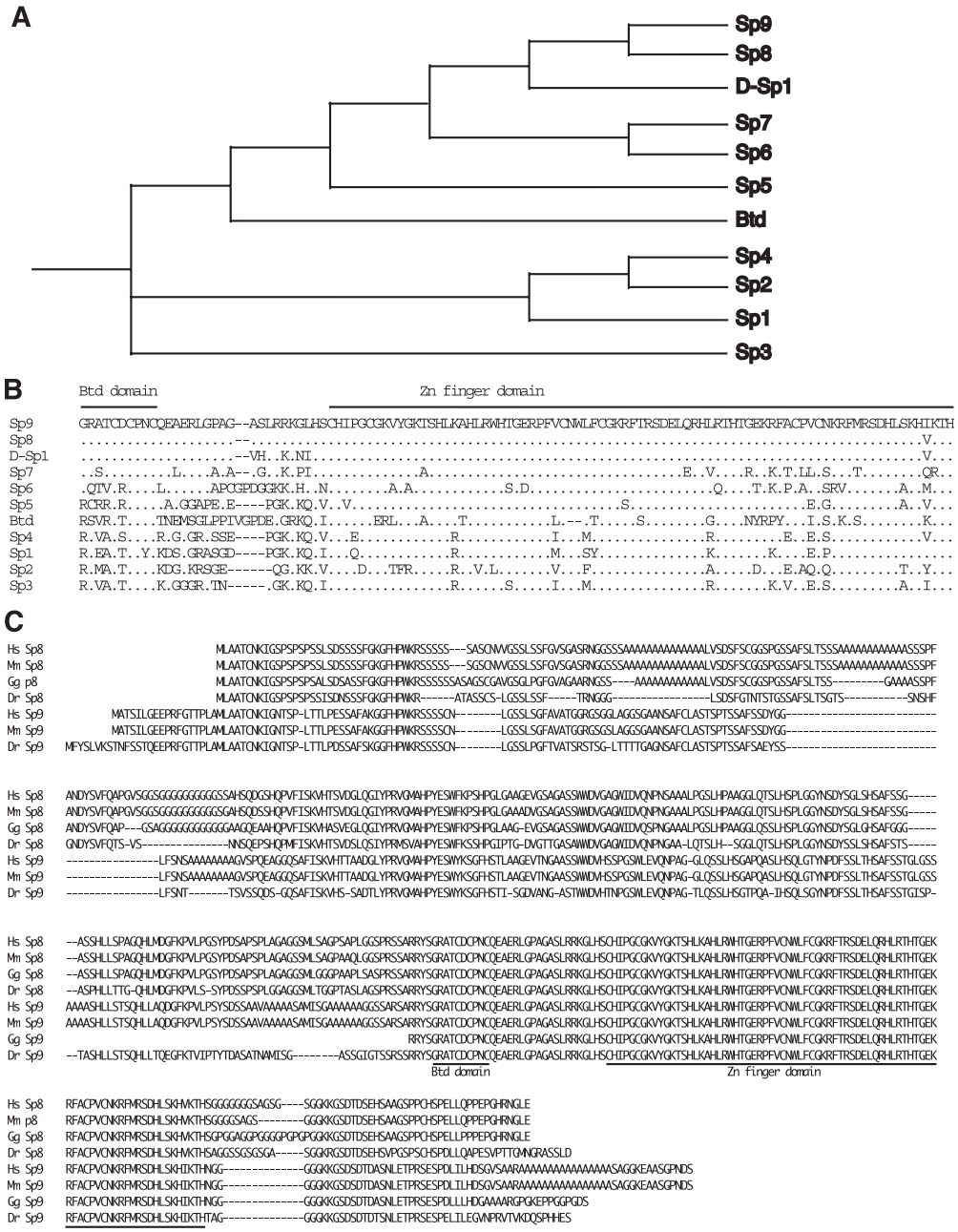

Fig. 1. Phylogenetic analysis and comparison of deduced amino acid sequences of the Sp family. (A) The deduced amino acid sequences of mouse Sp genes together with *Drosophila btd* and *Drosophila Sp1* are analyzed by CLUSTAL-W program. (B) Amino acid sequence alignment of the conserved region of the Sp family, from the *btd* domain to the Zn-finger domain. Identical residues, when compared with Sp9, are indicated by dots. Gaps in the sequence, indicated by dashes, are introduced to improve sequence alignment. The *btd* domain and Zn-finger domains are indicated by lines above the amino acid sequences. (C) Alignment of deduced amino acid sequences of *Sp8* and *Sp9* from human (*Homo sapiens*, Hs), mouse (*Mus musculus*, Mm), chick (*Gallus gallus*, Gg) and zebrafish (*Danio rerio*, Dr). The *btd* domain and the Zn-finger domains are indicated by lines.

from nucleotide position –1 to +24, relative to the translation start site: 5′-TTTGTTACACGTCGCAGCCAACATG-3′.

The zebrafish *sp9* morpholino sequence lies from nucleotide position –14 to +11, relative to the translation start site: 5′-CTATAAAACATAGCTGGCTTGTGTG-3′.

The standard control oligonucleotide available from GeneTools was used. The morpholinos were solubilized in 1×Danieu's solution and injected into one-cell stage zebrafish embryos at a range of 5-15 ng/embryo (Ng et al., 2002).

Results

Identification of two closely related Sp genes, *Sp8* and *Sp9*

In the course of our experiments to characterize clones involved in chick limb development, we isolated a clone expressed in the AER, which contained a *btd*-like Zn-finger domain. Screening cDNA libraries resulted in isolation of clones encoding three different *btd*-like genes, *Sp8*, *Sp5* and a novel Zn finger-containing clone. We termed this new clone chick *Sp9*, based on the fact the clone contains a *btd* domain and C2H2-type Zn-finger domain, characteristic domains conserved in Sp family members, and that its deduced amino acid sequence of the C-terminal region was different from that of *Sp8* (Fig. 1). Previous analysis, including a large-scale systematic characterization of mouse transcriptome, identified *Sp8* (Bouwman and Philipsen, 2002; Ravasi et al., 2003). The analyses, however, did not identify *Sp9*. To clarify whether *Sp9* exists in other vertebrates, we searched databases and found a mouse EST clone (Accession Number AW494427 in NCBI database) and a human sequence (hCT1831218 in Celera

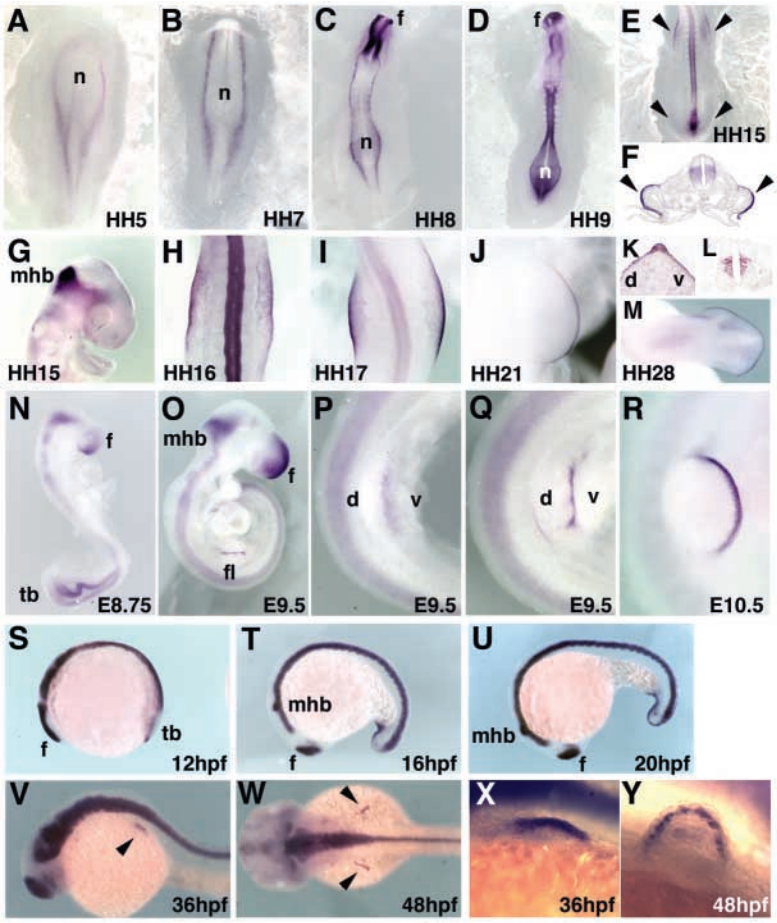

Fig. 2. Embryonic expression pattern of *Sp8* in chick, mouse and zebrafish. (A-M) Chick embryos showing expression of *Sp8* from dorsal views (A-E,H-J,M) with the anterior towards the top, a lateral view (G), and transverse sections (F,K,L). (N-R) Mouse embryos showing expression of *Sp8* from lateral views (N-Q) and a dorsal view (R). (S-Y) Zebrafish embryos showing *sp8* expression from lateral views (S-V,X,Y) and a dorsal view (W) with the anterior towards the left. Pre- and early-somitogenesis stage expression of chick *Sp8* was detected at HH stage 5 (A), stage 7 (B), stage 8 (C) and stage 9 (D). (E) *Sp8* expression in the surface ectoderm of the limb-forming field (arrowheads) at HH stage 15. (F) A 30 μm section of the embryo in (E) at the forelimb level, showing the expression in the surface ectoderm (arrowheads) and in the neural tube. (G) Head region of the embryo in E showing the expression in the MHB. *Sp8* expression in the surface ectoderm in the forelimb field at HH stage 16 (H) and stage 17 (I). (J) *Sp8* expression in the AER at HH stage 21. In situ hybridization on 14 μm sections at the forelimb level of a HH stage 21 embryo shows a signal in the AER and the surface ectoderm (K) and signal in the proliferating interneuron (L). *Sp8* expression in the forelimb AER at HH stage 28 (M). Mouse *Sp8* expression at E8.75 (N) and E9.5 (O). (P,Q) The signal in the forelimb-forming region was detected in the ventral ectoderm at E9.5. The embryonic stage in P is slightly earlier than that of Q. (R) Strong *Sp8* expression in the AER at E10.5. Zebrafish *sp8* expression at 12 hpf (S), 16 hpf (T) and 20 hpf (U). *sp8* expression in pectoral fin buds (arrowhead) at 36 hpf (V) and 48 hpf (W). The expression in the fin bud was observed in the apical fold at 36 hpf (X) and 48 hpf (Y). d, dorsal side; f, forebrain; fl, forelimb; mhb, midbrain/hindbrain boundary; n, Hensen's node; tb, tail bud; v, ventral side.

database). Based upon the deduced amino acid sequence, we concluded that these sequences encoded *Sp9* (Fig. 1). Subsequently, we screened a zebrafish cDNA library and obtained two closely related Zn finger-containing clones. Sequence analysis revealed that these clones show a high degree of similarity to the mouse *Sp8* and *Sp9* genes (Fig. 1C). Our analyses indicate that *Sp9* is a novel Zn finger containing *btd*-like factor expressed in human, mouse, chick and zebrafish.

We found that *Sp9* and *Sp3* are arranged in close proximity on mouse chromosome 2 (293 kb away) with their promoters facing each other, similar to *Sp8-Sp4* (chromosome 12), *Sp1-Sp7* (chromosome 15) and *Sp2-Sp6* (chromosome 11) (Bell et al., 2003). We also found that *Sp5* is located close to *Sp3*, but on the opposite side to where *Sp9* is located and also further away from *Sp3* than *Sp9* is (2564 kb). A similar gene arrangement was also observed with human *Sp1-Sp9* genes. The arrangement of Sp genes revealed that eight genes are arranged in a pair-wise manner on four different chromosomes, and *Sp5* appears to be in a position that is independent of the other Sp genes. This arrangement suggests that Sp genes arose from a common ancestor by tandem duplication and chromosomal duplication, as proposed for other gene families (Agulnik et al., 1996).

The highly homologous Zn finger domain made it difficult to compare amino acid sequences of Sp8 and Sp9 with other Sp family members within the domain (Fig. 1B). Phylogenetic analysis of deduced amino acid sequences of mouse *Sp1-Sp9* together with two *Drosophila* Sp family members, *btd* and *Sp1* revealed that mouse *Sp8* and *Sp9* are closely related to *Drosophila Sp1* (Fig. 1A). Sp8 contains characteristic Ser-rich, Ala-rich and Gly-rich stretches in its N-terminal domain. The zebrafish Sp8 is slightly different from the other Sp8 sequences in its N-terminal region, and is shorter than the others (Fig. 1C). The Sp9 sequence contains Ser-rich and Ala-rich domains in its N-terminal region; however, it does not contain the Gly-rich domain found in Sp8. Both Sp8 and Sp9 contain a Gly-rich sequence in the region 3′ to the Zn-finger domain. In all of the Sp8 and Sp9 sequences analyzed in this study, the amino acid sequences from the *btd* domain to the Zn-finger domain are identical except for one amino acid (Fig. 1B). The high degree of conservation of amino acid sequences among different species hints at their importance in vertebrate evolution.

Expression pattern of *Sp8* in chick, mouse and zebrafish embryos

In order to understand the roles of *Sp8* and *Sp9*, we first decided to analyze their embryonic expression pattern in chick, mouse and zebrafish embryos by in situ hybridization.

Sp8 expression was detected in early stages of chick embryos as an oval and 2 stripes at HH stage 5 (Fig. 2A), which became two lateral stripes at HH stage 7, running along the anteroposterior body axis from the head ectoderm to the anterior region of the primitive streak (Fig. 2B). At HH stage 8, strong expression in the anterior neuroectoderm, which forms the central nervous system, was observed (Fig. 2C), and

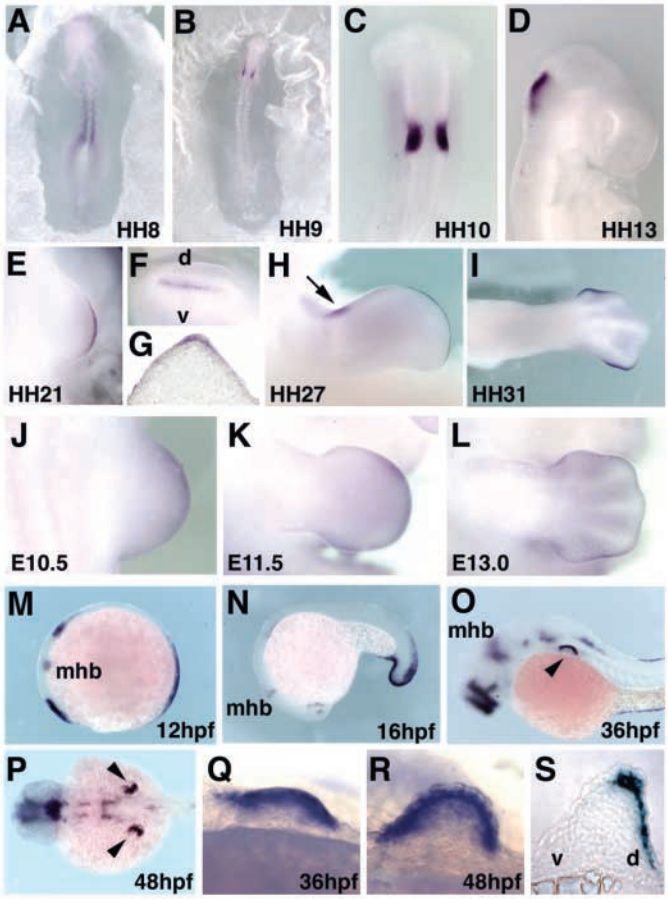

Fig. 3. Embryonic expression pattern of *Sp9* in chick, mouse and zebrafish. (A-I) Chick embryos showing expression of *Sp9* from dorsal views (A-C,E,H,I); a lateral view (D) with the anterior towards the top; a frontal view (F) with the dorsal towards the top; and a transverse section (G). (J-L) Mouse embryos showing expression of *Sp9* from dorsal views. (M-S) Zebrafish embryos showing *sp9* expression from lateral views (M-O,Q,R) and a dorsal view (P) with the anterior towards the left, and a transverse section (S). Chick *Sp9* expression at HH stage 8 (A), stage 9 (B), stage 10 (C) and stage 13 (D). (E,F) *Sp9* expression in the AER at HH stage 21. (G) Transverse section of the limb in E shows the signal in the AER and surface ectoderm. (H) *Sp9* is expressed in a small area in the anterior margin (arrow) in addition to the AER at HH stage 27. *Sp9* expression was restricted to the anterior and posterior edges of the autopod at HH stage 31 (I). Mouse *Sp9* was detected in the AER and the surface ectoderm at E10.5 (J), E11.5 (K) and E13.0 (L). Zebrafish *sp9* expression at 12 hpf (M) and 16 hpf (N). *sp9* expression in the pectoral fin (arrowhead) at 36 hpf (O,Q) and 48 hpf (P,R,S). (S) An 8 μm transverse section of the pectoral fin bud of the embryo in P, showing the *sp9* expression in the ectoderm. d, dorsal side; mhb, midbrain/hindbrain boundary; v, ventral side.

at HH stage 9, *Sp8* is expressed in the most anterior region of the forebrain, midbrain, neural groove and Hensen's node (Fig. 2D). The expression in the midbrain was later confined to the midbrain/hindbrain boundary, a signaling center that controls midbrain development (Fig. 2G) (Chi et al., 2003; Crossley et al., 1996a; Lee et al., 1997). At HH stage 15-16, the expression of *Sp8* was broadly observed in the surface ectoderm of the limb-forming fields (Fig. 2E,F, arrowheads), in addition to the neural tube. The signal in the neural tube marks proliferating neural cells, and is excluded from the dorsal and ventral region (Fig. 2F). The expression in the limb field became confined to the distal region of the limb at HH stage 16 and 17, with still scattered signal visible in the surface ectoderm of the limb bud (Fig. 2H,I). *Sp8* is strongly expressed in the AER and weakly in the ectoderm in the developing limb bud at HH stage 21 (Fig. 2J,K). At this stage, the neural tube expression was restricted to proliferating interneurons with a reversed triangle shape, and excluded from the dorsal-most and ventral-most regions (Fig. 2L). The expression in the AER was detected throughout later stages of limb development (Fig. 2M).

A similar expression pattern was observed in mouse and zebrafish embryos. Mouse *Sp8* expression was detected in the forebrain, midbrain/hindbrain boundary and neural tube (Fig. 2N,O; Bell et al., 2003; Treichel et al., 2003). At the stage of limb bud outgrowth, *Sp8* is expressed in a scattered manner in the ventral ectoderm (Fig. 2P,Q), and is later confined to the AER (Fig. 2R). In zebrafish, *sp8* was detected in the forebrain, prospective midbrain/hindbrain boundary, tail bud, and neural keel and neural tube in the somitogenesis stages (Fig. 2S-U). *sp8* is expressed in the pectoral fin bud, and the signal is restricted to the apical fold, a structure corresponding to the AER in chick and mouse embryos (Fig. 2V-Y).

Overall, the expression pattern of *Sp8* is conserved among the different vertebrate species studied. In particular, the expression in the limb buds, forebrain, midbrain/hindbrain boundary and neural tube suggests that *Sp8* has a conserved role in the development of these structures during mouse, chick and zebrafish embryogenesis.

Expression pattern of *Sp9* in chick, mouse and zebrafish embryos

Sp9 expression was not detected in early stages of chick development (HH stage 3-7). A strong signal was detected at HH stage 8 in the neural groove and anterior part of the regressing Hensen's node (Fig. 3A). *Sp9* expression showed a restricted pattern in the nervous system, like *Sp8*, but is excluded from the forebrain (Fig. 3B-D). The expression was detected in the anterior hindbrain (Fig. 3B,C), which will be confined to the midbrain/hindbrain boundary at HH stage 13 (Fig. 3D). In the developing limb, it is expressed in the AER and weakly in the distal surface ectoderm (Fig. 3E-G). Unlike *Sp8*, *Sp9* is expressed in a small area in the anterior border at HH stage 27 and later (Fig. 3H). After HH stage 28, expression in the AER disappears, and the transcripts start to be detected in the anterior and posterior edges of the autopod, but are excluded from the distal edge (Fig. 3I).

In mouse embryos, *Sp9* was detected in the AER during limb development as well as in the distal region of the ectoderm, in a similar manner to that of the chick (Fig. 3J-L). In zebrafish, *sp9* is expressed in the forebrain, unlike in the chick and mouse, and in the prospective midbrain/hindbrain boundary during early somitogenesis (Fig. 3M,N), which is narrower than that of *sp8*. As development proceeds, *sp9* is also detected in the hindbrain, as well as in the apical fold of the developing pectoral fin, and this expression extends proximally, as compared with that of *sp8* (Fig. 3O-R). A section of *sp9* hybridized embryos shows its strong expression in the basal stratum of the pectoral fin ectoderm (Fig. 3S) (Grandel and Schulte-Merker, 1998). Like *Sp8*, the conserved expression of

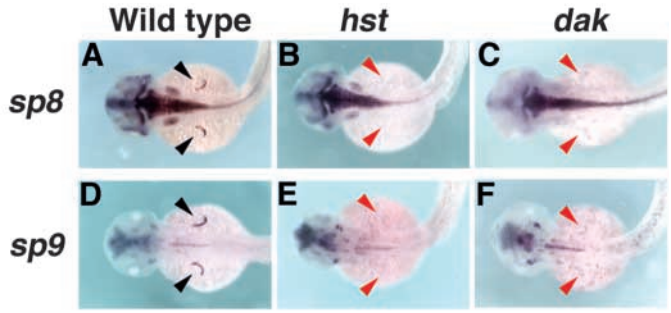

Fig. 4. Expression of *sp8* and *sp9* in the fin bud was downregulated in the zebrafish mutants with fin defects. (A-C) Dorsal views of the expression pattern of *sp8* at 40 hpf. (D-F) Dorsal views of the expression pattern of *sp9* at 40 hpf. (A) Expression of *sp8* in the pectoral fin bud of a wild type embryo (black arrowheads). The expression in the pectoral fin bud was downregulated (red arrowheads) in *hst* (B) and *dak* (C) mutants, while a normal expression in the neural tube was still detected. (D) Expression of *sp9* in the pectoral fin bud (black arrowhead) of a wild-type embryo. The expression in the pectoral fin bud was downregulated (red arrowheads) in *hst* (E) and *dak* (F) mutants, while a normal expression in the brain was still detected.

Sp9 in the AER in mouse, chick and zebrafish embryos alludes to the fact that *Sp9* may also have a key role during vertebrate limb development.

Mutant analysis indicates that expression of *Sp8* and *Sp9* correlates with proper limb outgrowth

It has recently been reported that *Sp8* has a role in maintaining *Fgf8* expression and limb outgrowth in mice (Bell et al., 2003; Treichel et al., 2003). In order to examine whether *Sp9* also has a role in limb development, as well as to examine possible molecular and genetic interactions of *Sp8* and *Sp9* with known signaling pathways involved in limb development, we made use of zebrafish pectoral fin mutants. We initially analyzed *hst* mutants, animals that bear a point mutation in the *tbx5*-coding sequence that results in a loss of function mutation (Garrity et al., 2002; Ng et al., 2002). Tbx5 is a mesenchymal factor required for limb bud initiation and outgrowth as an upstream regulator of *fgf10* in the pectoral fin field (Ahn et al., 2002; Ng et al., 2002). We observed significant downregulation of *sp8* and *sp9* expression in pectoral fin buds of *hst* mutants at 40 hpf (Fig. 4B,E), when compared with wild-type embryos (Fig. 4A,D). This result places *sp8* and *sp9* downstream of *tbx5* in limb development, and suggests that *sp9* as well as *sp8* must play a role in normal limb outgrowth. Similar results were obtained by using *nkl* mutant embryos (data not shown), which carry a mutation in the *raldh2* gene (Begemann et al., 2001). Given that *nkl* mutation lies upstream of tbx5 function in the pectoral fin formation, it further confirms that *sp8* and *sp9* are ectodermal factors downstream of mesenchymal signals.

We also studied *dak* mutant embryos, where fin buds start to grow but their outgrowth fails to be maintained (Grandel et al., 2000). We observed significant downregulation of *sp8* and *sp9* at 40 hpf when compared with wild-type embryos (Fig. 4C,F). This result further supports the involvement of *sp8* and *sp9* in fin outgrowth.

These analyses show that expression of *sp8* and *sp9* correlates with fin/limb development in zebrafish, and

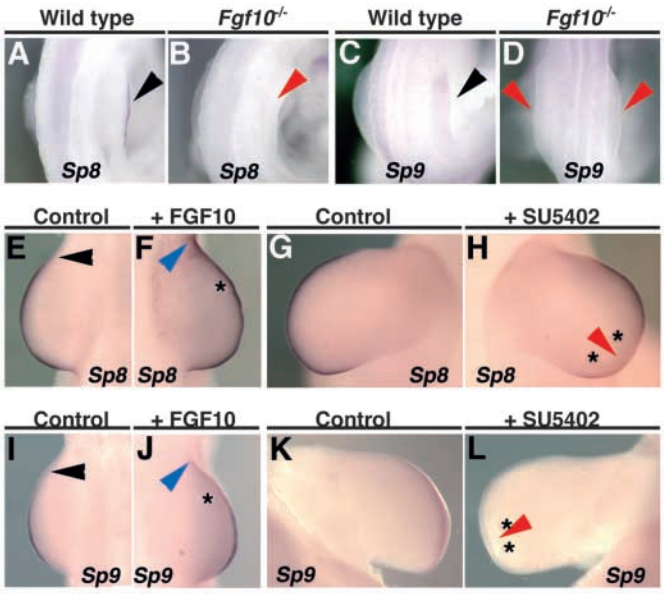

Fig. 5. Fgf10 signaling regulates *Sp8* and *Sp9*. Dorsal views of *Sp8* expression (A,B) and *Sp9* expression (C,D) in E9.5 mouse embryos. (E-H) Dorsal views of *Sp8* expression in chick limb buds. (I-L) Dorsal views (I,J) and ventral views (K,L) of *Sp9* expression in chick limb buds. All panels are with the anterior towards the top. (A-D) *Sp8* and *Sp9* expression detected in wild-type mouse embryos (A,C, black arrowheads), was significantly downregulated in *Fgf10*$^{-/-}$ embryos (B,D, red arrowheads). Implantation of Fgf10-soaked beads upregulated chick *Sp8* expression in the surface ectoderm and in the AER after 6 hours (F; compare with the contralateral control, E). Implantation of SU5402-beads downregulated expression of chick *Sp8* in the AER after 24 hours (red arrowhead in H; compare with the contralateral control, G). Implantation of Fgf10-beads upregulated chick *Sp9* expression in the surface ectoderm and in the AER after 6 hours (J; compare with the contralateral control, I). Implantation of SU5402-beads downregulated expression of chick *Sp9* in the AER after 24 hours (red arrowhead in L; compare with the contralateral control, K). Arrowheads in E,F and I,J indicate the anterior margin of the expression domain. The asterisks in F,H,J,L indicate implanted beads.

defects in fin/limb development are associated with their downregulation. The specific mutations in *hst* and *nkl* indicates that both *sp8* and *sp9* are ectodermal factors downstream of tbx5, a mesenchymal factor required for proper limb outgrowth.

Fgf10 signaling regulates both *Sp8* and *Sp9* expression

The Wnt and Fgf signaling pathways are two of the major pathways that positively control *Fgf8* expression in the AER (reviewed by Kato and Sekine, 1999; Martin, 1998; Tickle and Munsterberg, 2001; Yang, 2003). We therefore wanted to investigate whether the expression of *Sp8* and *Sp9* is regulated by these two signaling pathways.

Fgf10 is essential for inducing and maintaining *Fgf8* expression and AER formation during limb development. In order to analyze whether Fgf signaling also regulates expression of *Sp8* and *Sp9*, we first analyzed their expression in *Fgf10*$^{-/-}$ mouse embryos. We observed downregulation of *Sp8* and *Sp9* in embryos lacking *Fgf10* (Fig. 5A-D). This result

provides genetic evidence that initial induction of *Sp8* and *Sp9* in the ectoderm depends on Fgf10 signaling from the lateral plate mesoderm, and further confirms the result obtained by zebrafish pectoral fin mutant analysis (Fig. 4).

In order to examine the role of Fgf signaling in a spatially and temporally controlled manner, we carried out an experiment in which Fgf protein and the Fgf receptor inhibitor were applied in the developing chick limb. Implantation of beads soaked with Fgf10 in the anterior distal region of the limb resulted in upregulation of both *Sp8* and *Sp9* at 6 hours post-implantation (*n*=18/23 and 15/20 for *Sp8* and *Sp9*, respectively). The expression domain of *Sp8* and *Sp9* in the AER was extended in the Fgf10-bead-implanted limb, when compared with the contralateral control limb (Fig. 5E,F,I,J). In addition, both *Sp8* and *Sp9* were upregulated in the broad region exclusively in the limb ectoderm. We also examined the effect of Fgf8-soaked beads in the expression of *Sp8* and *Sp9* in the developing chick limb. However, we did not observe significant changes in their expression at 6 and 12 hours post-implantation (data not shown). These results indicate that Fgf10 signaling emanating from the mesenchyme is sufficient for expression of *Sp8* and *Sp9* in the ectoderm. To further examine the requirement of Fgf signaling in their expression in the AER, we implanted beads soaked with a Fgf receptor tyrosine kinase inhibitor, SU5402. Twenty-four hours post implantation, expression of *Sp8* and *Sp9* are significantly downregulated in close proximity to the beads (Fig. 5G,H,K,L, *n*=7/9 and *n*=6/8 for *Sp8* and *Sp9*, respectively). These results demonstrate that Fgf signaling is necessary and sufficient for expression of both *Sp8* and *Sp9* in the ectoderm.

Wnt signaling regulates *Sp8*, but not *Sp9* expression

Wnt3a, which signals through the β-catenin pathway, is expressed in the AER precursors and the established AER in the developing chick limb, and has been demonstrated to regulate *Fgf8* expression (Kawakami et al., 2001; Kengaku et al., 1998). In order to examine the role of the Wnt/β-catenin signaling pathway on *Sp8* and *Sp9* expression, we implanted cells expressing *Wnt3a* into the anterior distal tip of the chick limb bud at HH stage 19-21. This manipulation resulted in induction of ectopic expression of *Sp8* in the limb ectoderm in close proximity to the implanted cell pellet, at 6 and 12 hours post-implantation (*n*=2/6 at 6 hours, and *n*=5/6 at 12 hours; Fig. 6A,B). Moreover, retrovirus-mediated overexpression of dominant-active β-catenin resulted in ectopic induction of *Sp8* in a broad region of the chick limb ectoderm (*n*=5/5; Fig. 6C), which was associated with the formation of ectopic ridge-like structures (Fig. 6D). Contrary to what was observed with *Sp8*, we did not observe significant changes in the expression of *Sp9* in the limb ectoderm after the same experiments were performed (data not shown).

In mouse embryos, although *Wnt3a* is not expressed during limb development, another Wnt gene, *Wnt3* is expressed in the ectoderm and regulates limb development (Barrow et al., 2003). To further gain insights into the regulation of *Sp8* and *Sp9* expression by the Wnt/β-catenin signaling pathway, we performed the following experiments in mouse embryos. First, we used *Lrp6*$^{-/-}$ embryos for a loss-of-function approach. Lrp5/6 is a component of a Wnt-receptor complex that is required for canonical β-catenin-dependent signaling (He et al., 2004). We observed a variety of phenotypes in *Lrp6*$^{-/-}$ embryos, including total absence of limb bud outgrowth, severe truncation of limbs and truncations of the posterior part of the body. We chose embryos with no gross morphological defects, in order to avoid possible misinterpretation because of secondary effects. In E10.5 *Lrp6*$^{-/-}$ embryos, we observed downregulation of *Sp8* expression in the AER (Fig. 6E,F). Particularly, the domain of expression was shorter when compared with that of the wild-type limb. Second, we used *Dkk1*$^{-/-}$ embryos as a gain of function approach. Dkk1 is an extracellular Wnt antagonist, and β-catenin-dependent signaling is upregulated in *Dkk1*$^{-/-}$ embryos (Mukhopadhyay et al., 2001). We observed a stronger *Sp8* expression in the AER and ectopic *Sp8* expression outside the AER in 12.5 dpc *Dkk1*$^{-/-}$ embryos (Fig. 6G,H). However, in both *Lrp6*$^{-/-}$ and *Dkk1*$^{-/-}$ embryos, we did not observe significant changes in the expression of *Sp9* (data not shown). These results provide genetic evidence that Wnt/β-catenin signaling positively regulates *Sp8*, but not *Sp9*. Furthermore Wnt regulation of *Sp8*

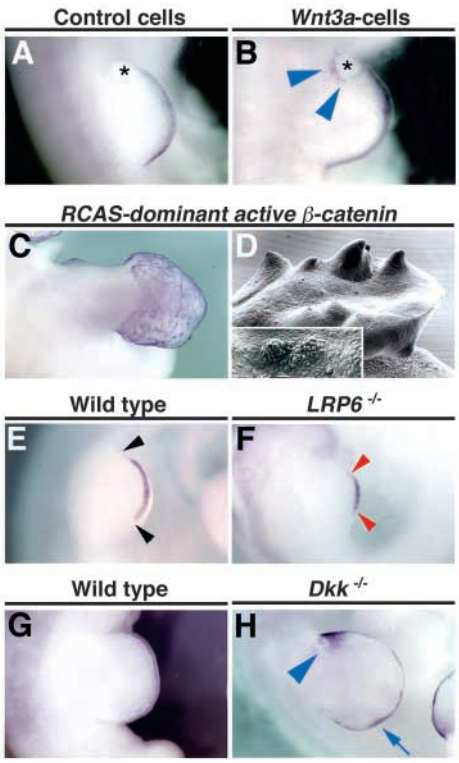

Fig. 6. Wnt signaling regulates *Sp8* expression. (A) Implantation of a control cell pellet had no effect on *Sp8* expression in the chick limb bud. (B) Implantation of a *Wnt3a*-expressing cell pellet induced *Sp8* expression in the ectoderm (arrowheads). Asterisks indicate pellets. (C) Injection of RCAS dominant-active β-catenin induced *Sp8* expression in the wide region of ectoderm. (D) Electron microscopic analysis of RCAS dominant-active β-catenin-injected limb. β-Catenin activity induced ectopic ridge-like spikes. The inset in D is a closer view of the ectoderm. (E,F) *Sp8* expression in the forelimb bud in wild-type (E) and *Lrp6*$^{-/-}$ (F) embryos at E10.5. The *Sp8* expression domain in E and F are labeled with black and red arrowheads, respectively. (G,H) *Sp8* expression in the forelimb bud in wild-type (G) and *Dkk1*$^{-/-}$ (H) embryos at E12.5. In *Dkk1*$^{-/-}$ embryos, the *Sp8* expression is stronger in the AER (blue arrow) and ectopically induced outside the AER (blue arrowhead).

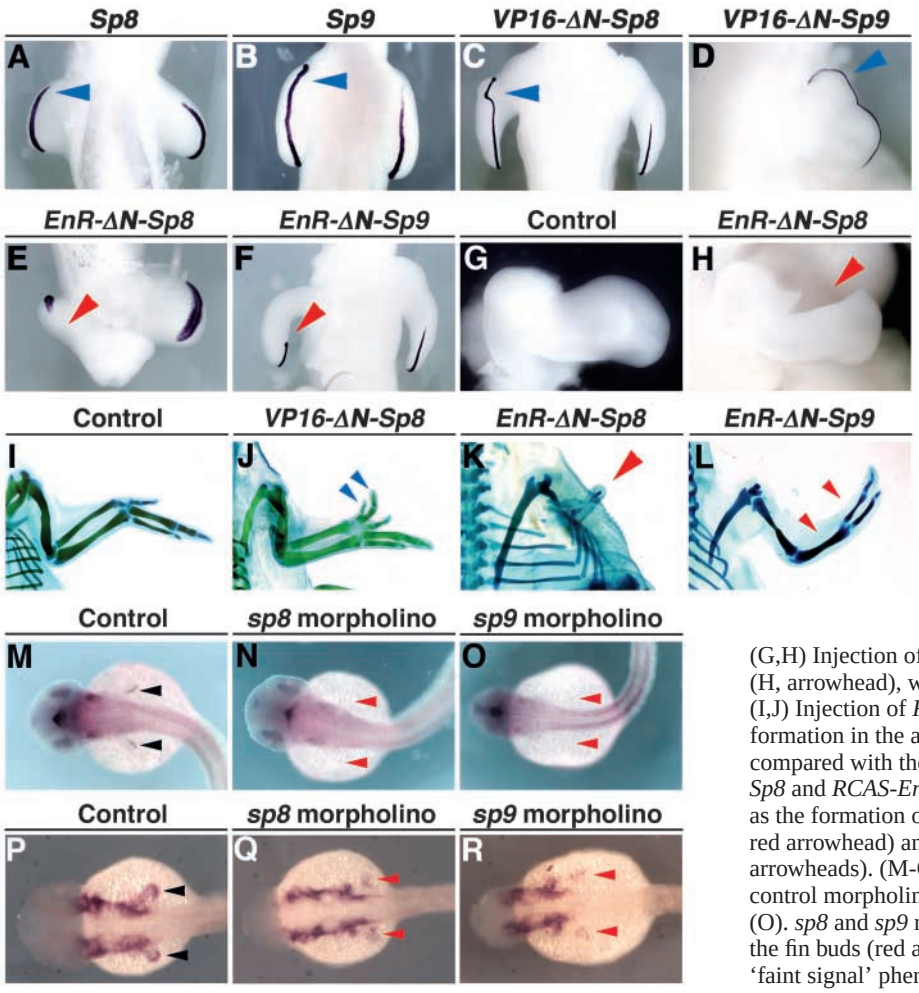

Fig. 7. *Sp8* and *Sp9* regulate *Fgf8* expression and limb outgrowth. Frontal views (A-C,E,F) and a dorsal view (D) of *Fgf8* expression in chick limb buds with the anterior towards the top. (G,H) Dorsal views of chick forelimbs with the anterior towards the top. (I-L) Dorsal views of chick forelimb skeletons. (M-R) Dorsal views of zebrafish embryos with the anterior towards the left. (A-F) Injection of virus was made on the right side; the left side serves as the contralateral control. Injection of *RCAS-Sp8* (A) and *RCAS-Sp9* (B) resulted in an expansion (arrowheads) of the *Fgf8* expression domain in the developing limb. Injection of *RCAS-VP16-ΔN-Sp8* (C) and *RCAS-VP16-ΔN-Sp9* (D) resulted in the elongation of the AER marked by the elongated expression domain (arrowheads) of *Fgf8*. Injection of *RCAS-EnR-ΔN-Sp8* (E) and *RCAS-EnR-ΔN-Sp9* (F) resulted in downregulation of *Fgf8* expression (arrowheads) in the limb. (G,H) Injection of *RCAS-EnR-ΔN-Sp8* caused an indentation (H, arrowhead), whereas control injection had no effect (G). (I,J) Injection of *RCAS-VP16-ΔN-Sp8* caused ectopic digit formation in the anterior domain (J, blue arrowheads) when compared with the control (I). (K,L) Injection of *RCAS-EnR-ΔN-Sp8* and *RCAS-EnR-ΔN-Sp9* caused hypoplasia of the limb, such as the formation of a small spike with unidentifiable elements (K, red arrowhead) and loss of cartilage elements (L, red arrowheads). (M-O) *fgf8* expression at 36 hpf injected with a control morpholino (M), *sp8* morpholino (N) and *sp9* morpholino (O). *sp8* and *sp9* morpholinos downregulated *fgf8* expression in the fin buds (red arrowheads). The embryos represent the typical 'faint signal' phenotype. (P-R) *prx1* expression in zebrafish injected with a control morpholino (P), *sp8* morpholino (Q) and *sp9* morpholino (R) at 36 hpf. *sp8* morpholino and *sp9* morpholino perturbed fin outgrowth, as visualized by *prx1* expression in the fin mesenchyme (red arrowheads).

appears to be a conserved feature in vertebrate limb development.

Sp8 and *Sp9* regulates *Fgf8* expression and limb outgrowth in vertebrates

To further investigate the roles of *Sp8* and *Sp9* during limb development, we used gain- and loss-of-function approaches by using viral-mediated expression in chick embryos. First, we overexpressed full-length *Sp8* and *Sp9* throughout the entire limb bud, and observed expansion of the AER marked by an expanded *Fgf8*-expressing domain (Fig. 7A,B). This phenotype was observed after overexpressing both *Sp8* and *Sp9* (n=3/17 and 10/60, for *Sp8* and *Sp9*, respectively). This result indicates that *Sp8* and *Sp9* can positively regulate *Fgf8* expression and AER morphology.

The role of *Sp8* and *Sp9* was also tested by using dominant-active and dominant-negative constructs in which *Sp8* and *Sp9* were fused to a VP16 or an EnR. We used a N-terminal-deleted form of *Sp8* (*ΔN-Sp8*) and *Sp9* (*ΔN-Sp9*) because of the transgene size limitation of RCAS system (~2 kb) and to avoid possible interferences resulting from the repetitive amino acid sequence in the N-terminal domain (which might interfere with the activity of these constructs). Injection of *RCAS-VP16-ΔN-Sp8* and *RCAS-VP16-ΔN-Sp9* resulted in a phenotype similar to that of full-length *Sp8* and *Sp9*. The distal region of the limb bud was enlarged and the AER was elongated (n=4/29 and n=4/42 for *VP16-ΔN-Sp8* and *VP16-ΔN-Sp9*, respectively; Fig. 7C,D). Correlating with the expansion of the distal mesenchyme phenotype, we observed ectopic digit formation in some of the affected embryos at later stages (n=3/25; Fig. 7J). These results show that *Sp8* and *Sp9* act as activators of *Fgf8* expression during limb development.

Next, we tried to examine the roles of *Sp8* and *Sp9* by a loss-of-function approach. Injection of *RCAS-EnR-ΔN-Sp8* and *RCAS-EnR-ΔN-Sp9* produced similar phenotypes, resulting in significant downregulation of *Fgf8* expression in the AER (n=3/15 and n=11/28 for *EnR-ΔN-Sp8* and *EnR-ΔN-Sp9*, respectively; Fig. 7E,F). This downregulation of *Fgf8* could lead to a partial loss of the AER, which was associated with an indentation phenotype in *RCAS-EnR-ΔN-Sp8*-injected embryos (Fig. 7G,H). Correlating with hypoplasia of the AER, we observed a variety of skeletal defects at later stages in *RCAS-EnR-ΔN-Sp8* or *RCAS-EnR-ΔN-Sp9* injected embryos. In the most severe cases, we observed a small projection (Fig. 7K). Where limbs should have formed, small cartilaginous rudiments were observed. The shoulder griddle, which is not

formed from the limb bud, appears normal. In the milder phenotypes, even though the limb was formed, it lacked several skeletal elements. Consistent with an indentation phenotype (Fig. 7H), Fig. 7L shows a phenotype lacking the radius and digit II. These results strongly support that both *Sp8* and *Sp9* may act to maintain the expression of key signaling molecules such as *Fgf8*, and the AER during limb development.

Because the frequency of phenotype is not very high (10-39%), we carefully examined virus infection using an *RCAS* probe in embryos injected with the aforementioned viruses. In 54-64% of embryos analyzed (*n*=28-44), we observed widely spread infection of RCAS viruses in the ectoderm, and widely spread strong mesenchymal infection was observed in 25-36% of the embryos. Some embryos showed a phenotype with only infection to the ectoderm (data not shown). This analysis, together with lack of phenotype produced by control *RCAS* virus (e.g. RCAS-alkaline phosphatase, *n*=60), indicates that the phenotype observed was specific for each virus injection experiment.

The high degree of amino acid sequence conservation between *Sp8* and *Sp9* raised the possibility that the VP16- and EnR-fusion constructs used, may act redundantly, and the phenotype observed could be not specific for *Sp8* or *Sp9*. To address this possibility, and also to avoid redundancy between *Sp8* and *Sp9*, we performed knock-down experiments in the zebrafish using morpholinos. The effects of *sp8* and *sp9* morpholinos on the development of the pectoral fin were analyzed using the *fgf8* and *prx1* markers. *prx1* is known to be expressed broadly in the chick limb bud mesenchyme in an AER-independent manner (Nohno et al., 1993), and was used to visualize the morphology of the developing pectoral fin in this study. Injection of either *sp8* morpholino or *sp9* morpholino resulted in downregulation of *fgf8* expression in the apical fold (Fig. 7M-O). As summarized in Table 1, we observed complete loss of *fgf8* expression in 10% of *sp9* morphants and very faint *fgf8* signal in 55% of morphants, resulting in *fgf8* downregulation in a total of 65% of *sp9* morphants at 36 hpf. *sp8* morphants showed milder phenotypes, and *fgf8* expression was downregulated in 33% of the *sp8* morphants. Fig. 7 shows the typical 'faint signal' phenotype, in which the signal is nearly invisible (Fig. 7M-O). Consistent with downregulation of *fgf8* expression, injection of either *sp8* morpholino or *sp9* morpholino resulted in interfering with pectoral fin outgrowth as visualized by expression of *prx1* (Fig. 7P-R). Moreover, we observed a synergistic effect of *sp8* morpholino and *sp9* morpholino on the expression of *fgf8*. Co-injection of *sp8* morpholino and *sp9* morpholino at a lower dose (5 ng each) resulted in downregulation of *fgf8* expression in ~80% of morphants. Increasing the amount of morpholinos (10 ng each) produced higher efficiency of downregulating *fgf8* expression, and *fgf8* expression was completely abolished in more than half of morphants.

These results clearly indicate that downregulation of function of either *sp8* or *sp9* is sufficient to downregulate *fgf8* expression and fin outgrowth. It also confirms the results observed in chick experiments with dominant-negative constructs, and further indicates that the coordinated actions of *sp8* and *sp9* might be required for *fgf8* expression in the zebrafish fin.

Discussion

Identification of a novel Sp family gene, *Sp9*

Large scale bioinformatic analyses have characterized Zn-finger transcription factors in the mouse transcriptome, including *Sp8* (Bouwman and Philipsen, 2002; Ravasi et al., 2003). Our experimental approach has identified an additional novel Zn finger transcription factor, *Sp9*, in human, mouse, chick and zebrafish, as well as *Sp8* in chick and zebrafish. The Sp family members are characterized by highly conserved *btd* domain and Zn-finger domain in their C-terminal region, which binds to the GC box on DNA. There is only one amino acid difference between Sp8 and Sp9 in these regions. Moreover, the amino acid sequence of this region is completely conserved among vertebrate species analyzed in this study. This high degree of sequence conservation during vertebrate evolution suggests not only that *Sp8* and *Sp9* may have essential roles, but also that they may have redundant activities. The existence of *Sp9* in invertebrates has not yet been reported. However, the identification of *Sp8* in the beetle as an essential factor for limb outgrowth (Beermann et al., 2004), and the fact that *Sp8* can functionally replace *btd* in *Drosophila* (Treichel et al., 2003) indicates that *Sp8/btd* has a common role in appendage development in vertebrates and invertebrates.

Evolution of Sp gene family

As previously demonstrated, the release of the mouse and human genome sequences revealed that Sp genes are arranged in a paired manner on chromosomes; *Sp1-Sp7*, *Sp2-Sp6* and *Sp4-Sp8*. Our analysis identified *Sp9* in close proximity to and in an opposite direction to *Sp3*. Based upon the arrangement of Sp genes on chromosomes, it is likely that a single primordial gene underwent a tandem duplication event and produced progenitor genes for the *Sp1-Sp4* subfamily and *Sp6-Sp9* subfamily. Then whole-cluster duplication(s) might have taken place to generate four Sp clusters. This is also supported by the proposal that the diversity of the amino acid sequences outside the Zn-finger domain were created by gene duplication (Kolell and Crawford, 2002). A similar scenario to gene evolution has been proposed for the *Tbx2* subfamily genes, *Tbx2-Tbx5* (Agulnik et al., 1996). Our finding that *Sp5* is not linked to other Sp genes supports a previously proposed evolutionary mechanism of Sp genes, in which *Sp5* might be an evolutionary link between the Sp family and *KLF* family,

Table 1. Summary of the effect of *sp8* morpholino and *sp9* morpholino on the expression of *fgf8* in the pectoral fin bud

Treatment	Dose	*n*	Percentage with complete loss	Percentage with faint signal	Percentage with normal
Control morpholino	15 ng	150	0	5	95
sp8 morpholino	15 ng	387	1	32	67
sp9 morpholino	15 ng	220	10	55	35
sp8 morpholino + *sp9* morpholino	5 ng of each	606	11	68	21
sp8 morpholino + *sp9* morpholino	10 ng of each	152	51	45	4

another Zn finger factor family whose primary structure of the Zn finger domain is related to that of Sp family but lacks the *btd* domain (Ravasi et al., 2003; Treichel et al., 2001).

Sp8 and *Sp9* are differentially regulated by Fgf and Wnt signaling

While necessity of *Sp8* for maintaining *Fgf8* expression in mice has recently been demonstrated, its placement in the genetic cascade that permits normal limb outgrowth and possible additional roles remained unknown. Furthermore, our identification of *Sp9*, a novel *btd*-like gene generated a new question: does *Sp9* have a similar or distinct role from *Sp8*? In order to try to address these issues and to gain insights into the mechanisms of *Sp8* and *Sp9* action, we analyzed their possible regulation by different signaling pathways known to play a key role during vertebrate limb development.

Genetic and embryological analyses have revealed that Fgf10-Fgfr2b in tandem is pivotal for inducing the expression of *Fgf8* in the AER precursor cells, migration of AER precursors from the surface ectoderm to the dorsoventral boundary, and formation of the AER (Gorivodsky and Lonai, 2003; Min et al., 1998; Ohuchi et al., 1997; Sekine et al., 1999). This also maintains expression of *Fgf8* in the AER in the established limb (Arman et al., 1999; Xu et al., 1998). Our analysis using *Fgf10*$^{-/-}$ embryos, as well as the manipulation of chick embryos, revealed that both *Sp8* and *Sp9* are ectodermal targets of Fgf10 signaling emanating from the mesenchyme during initiation and outgrowth of the limb bud (Fig. 5). This is supported by zebrafish mutant analysis, where retinoic acid and *tbx5* lie upstream of the *fgf10* signaling cascade in the mesenchyme (Begemann et al., 2001; Garrity et al., 2002; Ng et al., 2002). In these mutant embryos, *sp8* and *sp9* are significantly downregulated (Fig. 4), which further supports the fact that the regulation of *sp8* and *sp9* by mesenchymal signals is a conserved feature during vertebrate evolution.

In the ectoderm, Wnt/β-catenin signaling is known to be a crucial factor for induction and maintenance of *Fgf8* (reviewed by Yang, 2003). Unlike Fgf10, however, we observed differential regulation of *Sp8* and *Sp9* by Wnt/β-catenin signaling in both chick and mouse embryos (Fig. 6). Although we did not observe alteration of *Sp9* expression, *Sp8* expression was positively regulated by Wnt/β-catenin signaling. The fact that Fgf10 signaling and Wnt/β-catenin signaling can induce *Fgf8* in the ectoderm raised the possibility that activation of *Sp8* might be mediated through Fgf8 protein (Barrow et al., 2003; Kawakami et al., 2001; Kengaku et al., 1998; Ohuchi et al., 1997). This, however, does not seem to be the case, as exogenously applied Fgf8 could not induce *Sp8* and *Sp9*, while Fgf10 could. Our molecular and genetic analysis positions *Sp8* as a downstream factor of Fgf10 and Wnt/β-catenin, while *Sp9* is placed downstream of Fgf10, but independent of Wnt/β-catenin.

Sp8 and *Sp9* regulate *Fgf8* expression in the limb development

Our gain- and loss-of-function analyses have unveiled a role of *Sp9* and a new role of *Sp8* as positive regulators for *Fgf8* expression and AER formation. Our results with viral constructs of full length and VP16-fused forms of *Sp8* and *Sp9* strongly suggest that both genes are able to activate *Fgf8* expression as transcriptional activators (Fig. 7). This is also supported by the complementary results obtained using EnR fusion constructs and morpholinos. The fact that the proximal region of the *Fgf8* gene is GC-rich and includes several copies of consensus Sp1-recognition sequences (Brondani et al., 2002) further suggests that *Sp8* and *Sp9* directly regulate *Fgf8* expression in the limb.

During mouse embryogenesis, the precursors of the AER originate in the ventral ectoderm (Kimmel et al., 2000; Loomis et al., 1998). In the chick, these cells are distributed in the wide range of the surface ectoderm, both dorsally and ventrally (Altabef et al., 1997; Michaud et al., 1997). Interestingly, the distribution of *Sp8* transcripts at the time of *Fgf8* induction correlates with the appearance of the AER precursors. Expression of *Sp8* is detected in the AER precursors with a ventrally biased manner in mouse embryos (Fig. 2P,Q) (Bell et al., 2003; Treichel et al., 2003), and in a wide region of the surface ectoderm in chick (Fig. 2E,F). It has been demonstrated that *Fgfr2b*, the high-affinity receptor for Fgf10, is expressed widely in the surface ectoderm (Arman et al., 1999). The expression pattern of *Sp8*, together with the ability of *Sp8* and *Sp9* to induce *Fgf8* expression suggests that *Sp8* contributes to the initial induction of *Fgf8* in mouse and chick. Consistent with this, lower levels of *Fgf8* expression in the limb-forming area were observed in *Sp8*$^{-/-}$ embryos at E9.5, when *Fgf8* expression becomes evident in the limb-forming field (Treichel et al., 2003). The initial expression of *Fgf8* was not abolished completely in *Sp8*$^{-/-}$ embryos; however, this could be due to the redundant activity of *Sp9*. It will therefore be interesting to analyze double mutants of *Sp8* and *Sp9*.

Our data not only support the previously shown requirement of *Sp8* in the expression of *Fgf8* and limb outgrowth, but also demonstrate that *Sp9* is required for *Fgf8* expression and limb outgrowth. Our experiment with sequence-specific morpholinos excludes the possibility of redundant activity of the EnR fusion constructs (Fig. 7M-R). Therefore, the fact that downregulation of either *Sp8* or *Sp9* is sufficient to downregulate *Fgf8* expression and limb outgrowth, as well as the synergistic effects produced by co-injection of *sp8* morpholino and *sp9* morpholino on *fgf8* expression in zebrafish, strongly support the argument that these Sp factors may cooperate during normal limb outgrowth. A similar scenario could take place in other regions of the embryo where both genes are co-expressed, such as the midbrain/hindbrain boundary.

Conclusion

Vertebrate limb outgrowth requires proper activity of the AER. As such, induction and maintenance of the AER is a central issue for limb outgrowth and morphogenesis. Molecular and genetic approaches have revealed that *Fgf10*, *Wnt*/β-catenin and *Sp8* are crucial factors for these processes. Our studies have identified a novel *btd*-like transcription factor *Sp9*. Both *Sp8* and *Sp9* are regulated by Fgf10, and *Sp8* is additionally regulated by Wnt/β-catenin signaling. Furthermore, our results indicate that *Sp8* and *Sp9* mediate the induction and maintenance of *Fgf8* expression in the AER precursors and in the established AER, allowing proper limb/fin outgrowth in mouse, chick and zebrafish.

We thank May Schwarz for technical and editorial assistance. We also thank Carles Callol, Ilir Dubova, Hiroko Kawakami, Harley Pineda, Marina Raya and Gabriel Sternik for experimental assistance. We are most grateful to Dr Juan Hurle for electron microscopy images of RCAS-dominant-active β-catenin-injected embryos, to Dr Keisuke Sekine for his assistance and to Drs Naoyuki Wada, Setsuko Sahara and Ryuichi Shirasaki for the discussion. We express our appreciation to Dr Thomas Schilling for the zebrafish mutant *neckless*, and to Dr William C. Skarnes for the *Lrp6*$^{-/-}$ mouse. T.M. is partially supported by a fellowship from the Uehara Memorial Foundation and J.R.L. is supported by a fellowship from Fundação para a Ciencia e a Tecnologia. This work was supported by grants from FEDER to J.R.L.; and from the G. Harold and Leila Y. Mathers Charitable Foundation, the National Science Foundation and the National Institutes of Health to J.C.I.B.

References

Agulnik, S. I., Garvey, N., Hancock, S., Ruvinsky, I., Chapman, D. L., Agulnik, I., Bollag, R., Papaioannou, V. and Silver, L. M. (1996). Evolution of mouse T-box genes by tandem duplication and cluster dispersion. *Genetics* **144**, 249-254.

Ahn, K., Mishina, Y., Hanks, M. C., Behringer, R. R. and Crenshaw, E. B., III (2001). BMPR-IA signaling is required for the formation of the apical ectodermal ridge and dorsal-ventral patterning of the limb. *Development* **128**, 4449-4461.

Ahn, D. G., Kourakis, M. J., Rohde, L. A., Silver, L. M. and Ho, R. K. (2002). T-box gene tbx5 is essential for formation of the pectoral limb bud. *Nature* **417**, 754-758.

Altabef, M., Clarke, J. D. and Tickle, C. (1997). Dorso-ventral ectodermal compartments and origin of apical ectodermal ridge in developing chick limb. *Development* **124**, 4547-4556.

Arman, E., Haffner-Krausz, R., Gorivodsky, M. and Lonai, P. (1999). Fgfr2 is required for limb outgrowth and lung-branching morphogenesis. *Proc. Natl. Acad. Sci. USA* **96**, 11895-11899.

Barrow, J. R., Thomas, K. R., Boussadia-Zahui, O., Moore, R., Kemler, R., Capecchi, M. R. and McMahon, A. P. (2003). Ectodermal Wnt3/beta-catenin signaling is required for the establishment and maintenance of the apical ectodermal ridge. *Genes Dev.* **17**, 394-409.

Beermann, A., Aranda, M. and Schroder, R. (2004). The Sp8 zinc-finger transcription factor is involved in allometric growth of the limbs in the beetle Tribolium castaneum. *Development* **131**, 733-742.

Begemann, G., Schilling, T. F., Rauch, G. J., Geisler, R. and Ingham, P. W. (2001). The zebrafish neckless mutation reveals a requirement for raldh2 in mesodermal signals that pattern the hindbrain. *Development* **128**, 3081-3094.

Bell, S. M., Schreiner, C. M., Waclaw, R. R., Campbell, K., Potter, S. S. and Scott, W. J. (2003). Sp8 is crucial for limb outgrowth and neuropore closure. *Proc. Natl. Acad. Sci. USA* **100**, 12195-12200.

Bouwman, P. and Philipsen, S. (2002). Regulation of the activity of Sp1-related transcription factors. *Mol. Cell. Endocrinol.* **195**, 27-38.

Brondani, V., Klimkait, T., Egly, J. M. and Hamy, F. (2002). Promoter of FGF8 reveals a unique regulation by unliganded RARalpha. *J. Mol. Biol.* **319**, 715-728.

Capdevila, J. and Izpisua Belmonte, J. C. (2001). Patterning mechanisms controlling vertebrate limb development. *Annu. Rev. Cell Dev. Biol.* **17**, 87-132.

Capdevila, J., Tabin, C. and Johnson, R. L. (1998). Control of dorsoventral somite patterning by Wnt-1 and beta-catenin. *Dev. Biol.* **193**, 182-194.

Chi, C. L., Martinez, S., Wurst, W. and Martin, G. R. (2003). The isthmic organizer signal FGF8 is required for cell survival in the prospective midbrain and cerebellum. *Development* **130**, 2633-2644.

Crossley, P. H., Martinez, S. and Martin, G. R. (1996a). Midbrain development induced by FGF8 in the chick embryo. *Nature* **380**, 66-68.

Crossley, P. H., Minowada, G., MacArthur, C. A. and Martin, G. R. (1996b). Roles for FGF8 in the induction, initiation, and maintenance of chick limb development. *Cell* **84**, 127-136.

Dudley, A. T., Ros, M. A. and Tabin, C. J. (2002). A re-examination of proximodistal patterning during vertebrate limb development. *Nature* **418**, 539-544.

Garrity, D. M., Childs, S. and Fishman, M. C. (2002). The heartstrings mutation in zebrafish causes heart/fin Tbx5 deficiency syndrome. *Development* **129**, 4635-4645.

Gorivodsky, M. and Lonai, P. (2003). Novel roles of Fgfr2 in AER differentiation and positioning of the dorsoventral limb interface. *Development* **130**, 5471-5479.

Grandel, H. and Schulte-Merker, S. (1998). The development of the paired fins in the zebrafish (Danio rerio). *Mech. Dev.* **79**, 99-120.

Grandel, H., Draper, B. W. and Schulte-Merker, S. (2000). dackel acts in the ectoderm of the zebrafish pectoral fin bud to maintain AER signaling. *Development* **127**, 4169-4178.

Hamburger, V. and Hamilton, H. (1951). A series of normal stages in the development of the chick embryo. *J. Morph.* **88**, 49-92.

He, X., Semenov, M., Tamai, K. and Zeng, X. (2004). LDL receptor-related proteins 5 and 6 in Wnt/β-catenin signaling, Arrows point the way. *Development* **131**, 1663-1677.

Kato, S. and Sekine, K. (1999). FGF-FGFR signaling in vertebrate organogenesis. *Cell. Mol. Biol.* **45**, 631-638.

Kawakami, Y., Capdevila, J., Buscher, D., Itoh, T., Rodriguez Esteban, C. and Izpisua Belmonte, J. C. (2001). WNT signals control FGF-dependent limb initiation and AER induction in the chick embryo. *Cell* **104**, 891-900.

Kawakami, Y., Rodriguez-Leon, J., Koth, C. M., Buscher, D., Itoh, T., Raya, A., Ng, J. K., Esteban, C. R., Takahashi, S., Henrique, D. et al. (2003). MKP3 mediates the cellular response to FGF8 signalling in the vertebrate limb. *Nat. Cell Biol.* **5**, 513-519.

Kengaku, M., Capdevila, J., Rodriguez-Esteban, C., de la Pena, J., Johnson, R. L., Belmonte, J. C. and Tabin, C. J. (1998). Distinct WNT pathways regulating AER formation and dorsoventral polarity in the chick limb bud. *Science* **280**, 1274-1277.

Kimmel, R. A., Turnbull, D. H., Blanquet, V., Wurst, W., Loomis, C. A. and Joyner, A. L. (2000). Two lineage boundaries coordinate vertebrate apical ectodermal ridge formation. *Genes Dev.* **14**, 1377-1389.

Kolell, K. J. and Crawford, D. L. (2002). Evolution of Sp transcription factors. *Mol. Biol. Evol.* **19**, 216-222.

Lee, S. M., Danielian, P. S., Fritzsch, B. and McMahon, A. P. (1997). Evidence that FGF8 signalling from the midbrain-hindbrain junction regulates growth and polarity in the developing midbrain. *Development* **124**, 959-969.

Lewandoski, M., Sun, X. and Martin, G. R. (2000). Fgf8 signalling from the AER is essential for normal limb development. *Nat. Genet.* **26**, 460-463.

Loomis, C. A., Kimmel, R. A., Tong, C. X., Michaud, J. and Joyner, A. L. (1998). Analysis of the genetic pathway leading to formation of ectopic apical ectodermal ridges in mouse Engrailed-1 mutant limbs. *Development* **125**, 1137-1148.

Martin, G. R. (1998). The roles of FGFs in the early development of vertebrate limbs. *Genes Dev.* **12**, 1571-1586.

Michaud, J. L., Lapointe, F. and le Douarin, N. M. (1997). The dorsoventral polarity of the presumptive limb is determined by signals produced by the somites and by the lateral somatopleure. *Development* **124**, 1453-1463.

Min, H., Danilenko, D. M., Scully, S. A., Bolon, B., Ring, B. D., Tarpley, J. E., DeRose, M. and Simonet, W. S. (1998). Fgf-10 is required for both limb and lung development and exhibits striking functional similarity to Drosophila branchless. *Genes Dev.* **12**, 3156-3161.

Moon, A. M. and Capecchi, M. R. (2000). Fgf8 is required for outgrowth and patterning of the limbs. *Nat. Genet.* **26**, 455-459.

Mukhopadhyay, M., Shtrom, S., Rodriguez-Esteban, C., Chen, L., Tsukui, T., Gomer, L., Dorward, D. W., Glinka, A., Grinberg, A., Huang, S. P. et al. (2001). Dickkopf1 is required for embryonic head induction and limb morphogenesis in the mouse. *Dev. Cell* **1**, 423-434.

Ng, J. K., Kawakami, Y., Buscher, D., Raya, A., Itoh, T., Koth, C. M., Rodriguez Esteban, C., Rodriguez-Leon, J., Garrity, D. M., Fishman, M. C. et al. (2002). The limb identity gene Tbx5 promotes limb initiation by interacting with Wnt2b and Fgf10. *Development* **129**, 5161-5170.

Niswander, L. (2003). Pattern formation, old models out on a limb. *Nat. Rev. Genet.* **4**, 133-143.

Nohno, T., Koyama, E., Myokai, F., Taniguchi, S., Ohuchi, H., Saito, T. and Noji, S. (1993). A chicken homeobox gene related to Drosophila paired is predominantly expressed in the developing limb. *Dev. Biol.* **158**, 254-264.

Ohuchi, H., Nakagawa, T., Yamamoto, A., Araga, A., Ohata, T., Ishimaru, Y., Yoshioka, H., Kuwana, T., Nohno, T., Yamasaki, M. et al. (1997). The mesenchymal factor, FGF10, initiates and maintains the outgrowth of the chick limb bud through interaction with FGF8, an apical ectodermal factor. *Development* **124**, 2235-2244.

Ornitz, D. M., Xu, J., Colvin, J. S., McEwen, D. G., MacArthur, C. A., Coulier, F., Gao, G. and Goldfarb, M. (1996). Receptor specificity of the fibroblast growth factor family. *J. Biol. Chem.* **271**, 15292-15297.

Philipsen, S. and Suske, G. (1999). A tale of three fingers, the family of

mammalian Sp/XKLF transcription factors. *Nucleic Acids Res.* **27**, 2991-3000.

Pinson, K. I., Brennan, J., Monkley, S., Avery, B. J. and Skarnes, W. C. (2000). An LDL-receptor-related protein mediates Wnt signalling in mice. *Nature* **407**, 535-538.

Pizette, S., Abate-Shen, C. and Niswander, L. (2001). BMP controls proximodistal outgrowth, via induction of the apical ectodermal ridge, and dorsoventral patterning in the vertebrate limb. *Development* **128**, 4463-4474.

Ravasi, T., Huber, T., Zavolan, M., Forrest, A., Gaasterland, T., Grimmond, S. and Hume, D. A. (2003). Systematic characterization of the zinc-finger-containing proteins in the mouse transcriptome. *Genome Res.* **13**, 1430-1442.

Rowe, D. A., Cairns, J. M. and Fallon, J. F. (1982). Spatial and temporal patterns of cell death in limb bud mesoderm after apical ectodermal ridge removal. *Dev. Biol.* **93**, 83-91.

Sekine, K., Ohuchi, H., Fujiwara, M., Yamasaki, M., Yoshizawa, T., Sato, T., Yagishita, N., Matsui, D., Koga, Y., Itoh, N. et al. (1999). Fgf10 is essential for limb and lung formation. *Nat. Genet.* **21**, 138-141.

Soshnikova, N., Zechner, D., Huelsken, J., Mishina, Y., Behringer, R. R., Taketo, M. M., Crenshaw, E. B., III and Birchmeier, W. (2003). Genetic interaction between Wnt/beta-catenin and BMP receptor signaling during formation of the AER and the dorsal-ventral axis in the limb. *Genes Dev.* **17**, 1963-1968.

Sun, X., Mariani, F. V. and Martin, G. R. (2002). Functions of FGF signalling from the apical ectodermal ridge in limb development. *Nature* **418**, 501-508.

Tickle, C. (2002a). Molecular basis of vertebrate limb patterning. *Am. J. Med. Genet.* **112**, 250-255.

Tickle, C. (2002b). Vertebrate limb development and possible clues to diversity in limb form. *J. Morphol.* **252**, 29-37.

Tickle, C. and Munsterberg, A. (2001). Vertebrate limb development – the early stages in chick and mouse. *Curr. Opin. Genet. Dev.* **11**, 476-481.

Treichel, D., Becker, M. B. and Gruss, P. (2001). The novel transcription factor gene Sp5 exhibits a dynamic and highly restricted expression pattern during mouse embryogenesis. *Mech. Dev.* **101**, 175-179.

Treichel, D., Schock, F., Jackle, H., Gruss, P. and Mansouri, A. (2003). mBtd is required to maintain signaling during murine limb development. *Genes Dev.* **17**, 2630-2635.

Vogel, A., Rodriguez, C. and Izpisua-Belmonte, J. C. (1996). Involvement of FGF-8 in initiation, outgrowth and patterning of the vertebrate limb. *Development* **122**, 1737-1750.

Wada, N., Kawakami, Y. and Nohno, T. (1999). Sonic hedgehog signaling during digit pattern duplication after application of recombinant protein and expressing cells. *Dev. Growth Differ.* **41**, 567-574.

Xu, X., Weinstein, M., Li, C., Naski, M., Cohen, R. I., Ornitz, D. M., Leder, P. and Deng, C. (1998). Fibroblast growth factor receptor 2 (FGFR2)-mediated reciprocal regulation loop between FGF8 and FGF10 is essential for limb induction. *Development* **125**, 753-765.

Yang, Y. (2003). Wnts and wing, Wnt signaling in vertebrate limb development and musculoskeletal morphogenesis. *Birth Defects Res. Part C Embryo Today* **69**, 305-317.